

Research Paper

Microstructural Investigation and Wear Characteristics of Al-Si-Ti Cast Alloys

Akeel Dhahir SUBHI¹*, Ali Abbar KHLEIF¹), Qasim Saad ABDUL-WAHID²)

¹⁾ *Department of Production Engineering and Metallurgy
University of Technology*

Baghdad, Iraq

*Corresponding Author e-mail: 70071@uotechnology.edu.iq

²⁾ *Materials Engineering Department
University of Al-Qadisiyah*

Diwaniya, Iraq

Hypoeutectic Al-7Si alloys containing various titanium proportions (0.8–1.6%) were produced and analyzed in this work. The wear characteristics of Al-Si alloys were studied under the conditions of dry sliding at various applied loads. Optical microscope (OM), scanning electron microscopy (SEM) and X-ray diffraction (XRD) were used to depict the microstructure, worn surface and phases, respectively. Phases of α -Al, eutectic and Ti9Al23 were recognized in the Al-Si-Ti alloys matrix. Considerable coarsening took place in α -Al and eutectic silicon in a fully eutectic through solidification. The hardness was increased as the titanium proportion increased. Furthermore, significant changes were found in the wear rate depending on the titanium proportion added and load applied.

Key words: hypoeutectic Al-Si alloy; microstructural investigation; intermetallic compound; wear characteristics.

1. INTRODUCTION

The mechanical, tribological and physical properties of aluminum alloys are important in the strategic/optimized combination of such alloys compared to other alloys. These properties give aluminum alloys great industrial significance including high specific strength, high temperature strength, wear resistance, good stiffness, good damping capacity and controllable coefficient of thermal expansion [1–4].

Aluminum-silicon alloys are one of the most remarkable aluminum alloys owing to their good general properties such as good casting properties in addition to good resistance to wear and corrosion [5, 6]. Cast hypoeutectic Al-Si alloys have many applications, especially in the manufacture of engine blocks, pistons,

pumps, automatic transmission's components and compressors [7–10]. Hardness is an important characteristic of wear control, as the wear resistance of a material increases as its hardness increases. Therefore, improving the wear resistance of Al-Si alloys requires a hard phase in the matrix regardless of whether they are cast or plastically deformed [11–13].

SAHEB *et al.* [14] observed that titanium addition to the cast and heat-treated Al-12Si alloy caused Al_3Ti precipitation, which enhanced wear resistance due to increased hardness. ZEREN and KARAKULAK [15] noted that the increased Ti proportion increased the hardness of Al-13.1Si alloy via the presence of intermetallic compounds, especially Al_3Ti , which appeared as petals and flakes relying upon the conditions of solidification applied. The impact of Si and Ti addition on the TiAlSi intermetallic properties was studied by GAO *et al.* [16]. They found that the microhardness and Si in flake-like TiAlSi intermetallic increased with the increase in Si proportion. GHOMASHCHI [17] showed that high solidification cooling rates and low titanium proportion in A356 Al alloy encouraged the formation of flake morphology of Ti based intermetallics instead of blocky morphology appearing at low solidification cooling rate and high titanium proportion. The properties of Al-Si alloys containing titanium and boron were investigated by KIM *et al.* [18]. They concluded that greater hardness and minimum wear rate were acquired in the Al-12Si-2.3Ti-1B alloy via the presence of Al_3Ti and $(\text{AlTi})\text{B}_2$ strengthening phases in comparison with other types of Al-Si alloys.

The investigation of microstructural evolution of Al-Si alloys requires further research, especially with the addition of different titanium proportions. Notably, the impact of Ti-based intermetallics on the wear properties was seldom investigated in Al-Si alloys containing titanium. Thus, we aimed in this research to study the impact of the addition of different Ti proportions on the microstructural evolution, hardness and wear characteristics of hypoeutectic Al-7Si alloy.

2. MATERIALS AND TESTING

Starting materials such as pure Al and master alloys of Al-11Si and Al-5Ti, whose chemistries are presented in Table 1, were used in this research. Various Al-Si alloys were manufactured by controlling the pure aluminum and Al-5Ti master alloy added to the Al-11Si master alloy. The different proportions of titanium added as Al-5Ti master alloy were 0.8, 1.3, and 1.6%. Binary Al-7Si alloy and Al-Si-xTi alloys were melted using graphite crucible in an electric furnace and poured into a heated copper mold (300°C) at 700°C and 1050°C, respectively. Coveral flux was utilized to preclude the molten absorption effect of gasses. The chemistries of Al-Si alloys prepared for investigation are illustrated in Table 2.

Table 1. Typical chemical compositions of starting materials used (mass fraction, %).

Alloy	Si	Fe	Cu	Mg	Ti	Al
Pure Al	0.214	0.095	0.036	0.004	0.001	balance
Al-11Si master alloy	10.83	0.981	0.980	0.263	0.033	balance
Al-5Ti master alloy	0.181	0.245	0.023	0.010	5.000	balance

Table 2. Typical chemical compositions of the investigated aluminum alloys (mass fraction, %).

Alloy	Si	Fe	Cu	Mg	Ti	Al
Al-7Si alloy	7.39	0.684	0.20	0.130	0.022	balance
Al-7Si-0.8Ti alloy	7.13	0.684	0.29	0.144	0.815	balance
Al-7Si-1.3Ti alloy	7.11	0.688	0.34	0.114	1.300	balance
Al-7Si-1.6Ti alloy	7.00	0.699	0.35	0.018	1.610	balance

Metallographic investigation of Al-Si alloys was achieved by employing grinding with various grades of SiC abrasive papers and polishing by utilizing 5 μm alumina slurry. The etching was performed by employing a 0.5%HF etching solution. Optical microscope (OM) was utilized to examine all prepared Al-Si alloys. The phases of Al-Si alloys were identified by employing the XRD instrument type 6000 Shimadzu with 30 mA current and 40 kV voltage. Copper target with 1.54 \AA wavelength was used during the XRD test.

The dry sliding wear experiments of Al-Si alloys were achieved utilizing pin-on-disk wear apparatus in air at room temperature (30–35°C). The pin was loaded onto a flat rotating disk (counterface) so that a circular wear path could be described. An AISI 1045 steel disk of 35 HRC with 510 rpm rotational speed was used as a counterface. The pins were positioned at a diameter (wear track diameter) of 18 cm on the counterface and had the dimension ϕ (10 mm) \times h (20 mm) (cylindrical specimen). Wear testing of all Al-Si alloys specimens was conducted at 20 min duration using 288.4 m/min sliding speed and normally applied loads of 5, 10, 15, 20, and 25 N that correspond to apparent contact pressures of 63.6, 127.3, 190.9, 254.6, and 318.3 kPa, respectively. The counterface surface was cleaned before conducting each test by employing SiC abrasive paper of 500 grade and alcohol. The pin surface that held against the counterface was prepared using grinding with 320, 500 and 1000 SiC abrasive papers sequentially followed by 5 μm alumina slurry polishing. Wear rates were estimated from the results reflecting the wear mass loss. An electronic balance with 0.0001 gm accuracy was used to measure the mass loss through wear testing. The pins were completely cleaned using acetone before wear testing. The wear rates were obtained by $W_r = \Delta w/S_d$, where W_r refers to the wear rates in gm/cm, Δw is the weight loss measured in grams and S_d is the sliding distance (576796.4 cm).

TESCAN SEM of high spatial resolution was used to obtain important information about the surface topography of worn surface using a focused electron beam of high energy to determine wear mechanism.

3. RESULTS AND DISCUSSION

3.1. Microstructure and hardness of Al-Si alloys

The optical micrograph of Al-Si cast alloys containing various titanium proportions illustrated that α -Al was grown in a dendritic manner and associated with eutectic (α -Al and Si) in the matrix (Fig. 1). The intermetallic compound of Ti_9Al_{23} was evolved via titanium addition. These phases were identified by employing XRD, where the phases of α -Al and Ti_9Al_{23} were observed at the same peak (Fig. 2). The d -spacings of α -Al at diffraction planes of (200) and (220) were 2.024 and 1.431 Å, respectively. These d -spacings were close to the d -spacings of 2.092 and 1.414 Å for Ti_9Al_{23} obtained at diffraction planes of (0016) and (2016), respectively. Therefore, the major convergence between the two phases d -spacing of α -Al and Ti_9Al_{23} was the essential cause of overlap. The Ti_9Al_{23} was evident as flakes and blokes in various morphologies in the matrix of Al-7Si cast alloys with Ti (Fig. 1). It appeared that flake Ti_9Al_{23} could be recognized obviously with increasing titanium proportion. It was clearly noticed the coarsening of α -Al and eutectic silicon in eutectic, especially in titanium contained Al-Si alloys, compared to the binary Al-7Si alloy. This could be related to the impact of pouring temperature, where the high pouring temperature increased

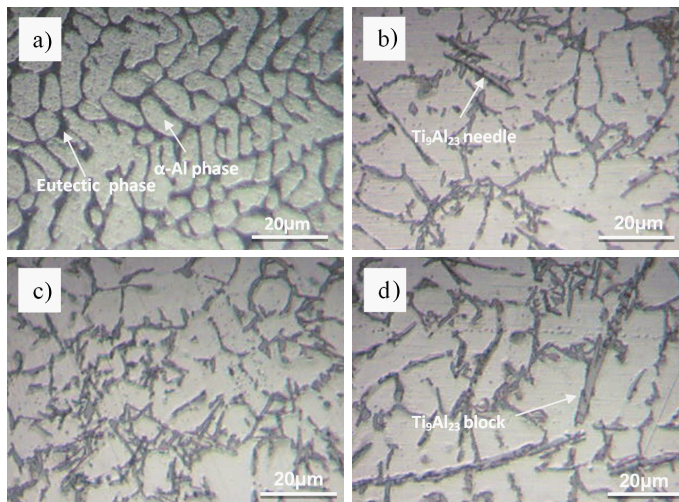


FIG. 1. Optical micrograph showing the solidification microstructure of (a) binary Al-7Si alloy containing (b) 0.8%Ti, (c) 1.3%Ti, (d) 1.6%Ti.

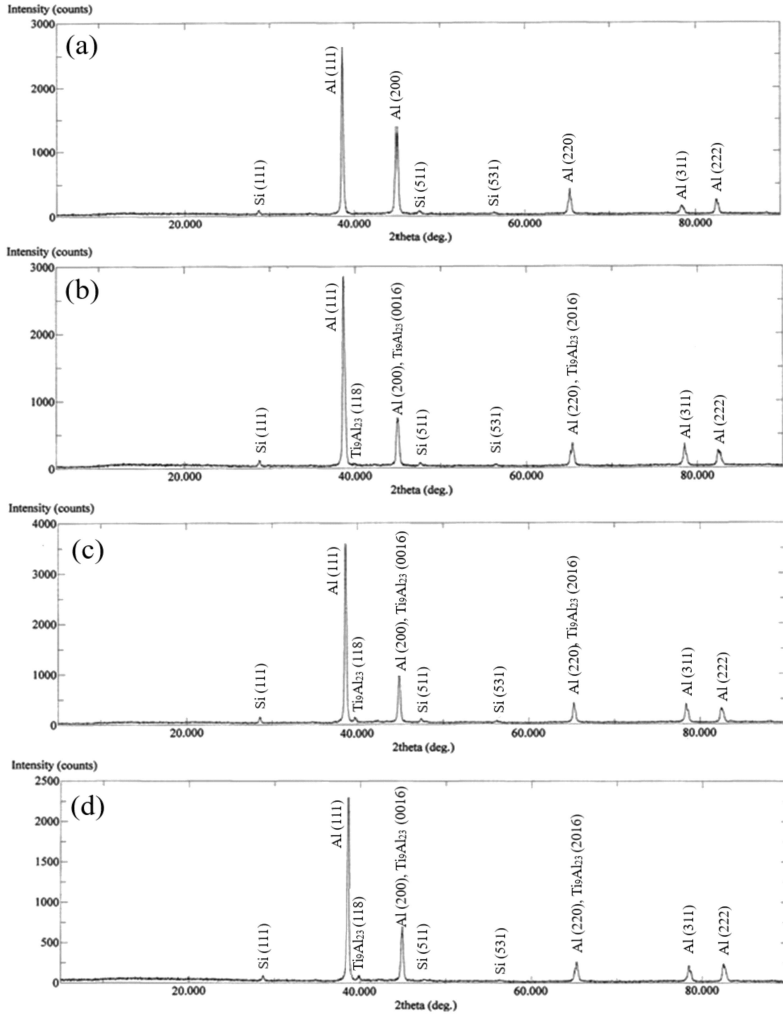


FIG. 2. XRD patterns of (a) binary Al-7Si alloy containing (b) 0.8%Ti, (c) 1.3%Ti, (d) 1.6%Ti.

the solidification time and hence coarsened the structure. The average size of α -Al *versus* Ti proportion is illustrated in Table 3.

Table 3. The average size of α -Al *versus* Ti proportion in Al-7Si alloy.

Ti [%]	Average size of α -Al [μ m]
0.022	8
0.815	13
1.30	11
1.61	16

The impact of the increased titanium proportion on the hardness of Al-7Si alloy is shown in Fig. 3. It appears that the titanium addition had a considerable impact on changing the hardness of the Al-7Si alloy as the increase in the titanium proportion led to an increment in the hardness. This could be related to the Ti_9Al_{23} that hindered dislocations motion.

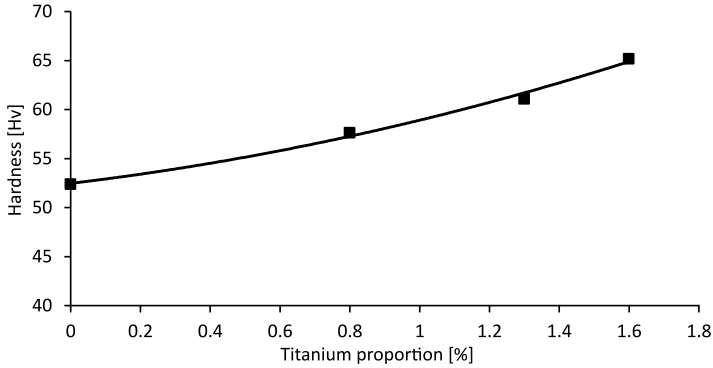


FIG. 3. Hardness *versus* Ti proportion for Al-7Si alloy.

3.2. Wear characteristics of Al-Si alloys

Researchers have conducted studies to determine the correlation between wear rate and applied load for metals and alloys and analyze the wear behavior during dry sliding. In this study, Fig. 4 shows the wear rate *versus* the applied load for the Al-Si cast alloys. It is evident that the increase in titanium proportion reduced the wear rate via Ti_9Al_{23} formation, which in turn had a significant impact on increasing the hardness. In general, wear resistance could be enhanced with increased hardness [19]. Therefore, as the titanium proportion increased, the wear rate started to lessen.

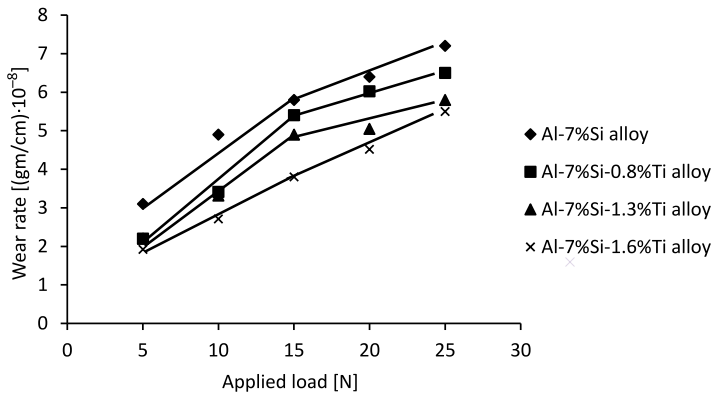


FIG. 4. Wear rate *versus* applied load for Al-Si alloys containing different proportions of Ti.

Moreover, the wear rate was increased with an increment in the applied load. Clearly, the transition from oxidative-metallic into metallic wear took place in aluminum-silicon alloys at a specified applied load of 15 N. This is demonstrated by the sharp rise in the curve slope of the wear rate *versus* applied load (Fig. 4). This means that a wear mechanism was initially oxidative-metallic but became metallic only during the wear tests under a sufficiently higher applied load (greater than 15 N). At first glance, there was no change in the slope of the Al-7Si-1.6Ti alloy. From the naked-eye observation of the worn surface of Al-7Si-1.6Ti alloy, it was noticed that the onset of metallic wear was at 15 N applied load. This was determined by shiny appearance that completely covered the worn surface, indicating the formation of metallic wear. The plastic deformation of the surface asperities was increased through sliding with the increased applied load, which in turn resulted in an increment in the actual contact area among the mating surfaces of the pin and the counterface.

The weak contact at the mating surfaces resulted in oxidative wear at the applied load below 15 N. The oxidative wear was caused by the oxidizing surface asperities of the pins. Fracture and compacting of the oxidized wear debris under dry sliding conditions occurred among the mating surfaces. This oxide layer, as investigated by SHIVANATH *et al.* [20], was formed in the range of (10–80 μm). Material removal from the surface of Al-Si alloys at a applied load greater than 15 N was predominantly achieved by the metallic wear mechanism, where the worn surface was manifested by plastic deformation and fracture. It could be postulated that the onset of plastic deformation was intensified in the surface asperities, which led to an increase in the dislocations density and consequently made the pin surface brittle [21]. This brittleness resulted in small cracks in the subsurface during dry sliding that expanded and extended toward the outer surface under the impact of the applied load to form metallic wear debris.

In all dry sliding wear tested Al-Si alloys, two wear regimes were recognized. The mechanisms that control the wear rate in each wear regime vary greatly. The features of each regime were easily recognized through the naked-eye observation, which made it easier to observe the wear transition. The first regime was a combination of two wear types, oxidative and metallic. Oxidative wear was distinguished by dark wear grooves due to the filling of these grooves with oxide debris of small particles. Metallic wear was characterized by shiny grooves and metallic luster. Surface oxidation, plastic deformation and delamination were the main damage characteristics of this regime. The wear rates of Al-Si alloys varied in this regime. The wear rate was equal or greater than $1.92 \cdot 10^{-8}$ gm/cm for Al-7Si-1.6Ti alloy and lower than $5.8 \cdot 10^{-8}$ gm/cm for Al-7Si alloy. The second regime was distinguished by gross plastic flow and deep grooves on the worn surface of Al-Si alloys. The wear rate was increased in this regime, and the worn surface had a shiny appearance due to metallic removal. Severe plastic defor-

mation and delamination were the main damage characteristics during the dry sliding of this regime. The wear rates of Al-Si alloys in the second regime varied between greater than $3.8 \cdot 10^{-8}$ gm/cm for Al-7Si-1.6Ti alloy and $7.2 \cdot 10^{-8}$ gm/cm for Al-7Si alloy. Moreover, Al-Si alloys wear-tested in this regime were characterized by transferring material from the pin surface to the counterface, which consequently increased the counterface surface roughness and wear rate due to an increment in the asperities overlap among the mating surfaces. No evidence was identified for the material back transfer during dry sliding from the counterface surface to the pin.

3.3. Worn surface study of Al-Si alloys

Worn surface topography study can provide a better understanding of the wear mechanism. The worn surface characterization using SEM for Al-Si alloys at 25 N applied load (Fig. 5) showed the roof tile laminates to be the essential characteristic of the worn surface. Distinct laminated layers were recognized

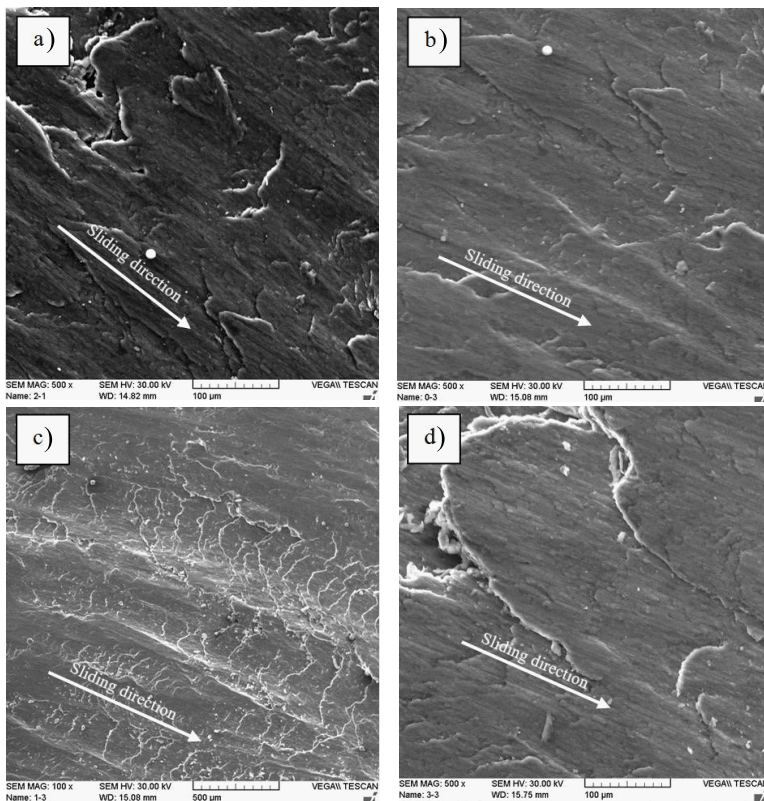


FIG. 5. Comparison of SEM worn surface images of Al-7Si alloy (a and b) and Al-7Si-0.8Ti alloy (c and d) under 25 N applied load.

clearly on the worn surface of tested Al-Si alloys. The interaction among the asperities of the pin surface and the counterface and adhesion effects may be responsible for creating laminated layers. Generally, delamination was a wear mechanism associated with surface fatigue where the sliding induced subsurface cracks were grown gradually and sheared to the surface to create delaminated layers. The delamination during dry sliding from the pin surface was constantly correlated with adhesion effects and material plastic flow. Additionally, few small dimples were recognized on the worn surface of Al-Si alloys and they were associated with delaminated layers. CLARKE and SARKAR [22] found that these dimples are characteristics of ductile fracture and related to the junctions adhesion and cold welding between the pin and the counterface where the only way to detach them is by breaking the junctions. The smooth worn surface of Al-Si alloys and fine particle-like debris adherent on it indicated that these particles were responsible for making fine grooves. The topography of a thin peninsula of material ready to detach as a thin plate indicated that its formation was dependent on the set of loads applied, materials' chemistries and the occurrence of plastic deformation (Fig. 5d).

4. CONCLUSION

Adding titanium to the Al-7Si alloy matrix resulted in Ti_9Al_{23} intermetallic compound formation. The formation of Ti_9Al_{23} was associated with the phases of α -Al and eutectic, where Ti_9Al_{23} appeared in various morphologies as flake and block. A significant impact related to the adding of titanium on increasing the hardness of Al-7Si alloys was identified by the formation of Ti_9Al_{23} . The increase in the titanium proportion resulted in the wear rate decrease due to the enhanced hardness of the Al-Si alloys. The two wear regimes distinguished in Al-Si cast alloys during dry sliding were oxidative-metallic and metallic wear, where the transition between them occurred at 15 N applied load. Several wear mechanisms contributed to degrading the surface of Al-Si alloys and delamination was responsible for the major portion of failure. Finally, we suggest that more in-depth investigations need to be carried out on this work.

REFERENCES

1. DAS S., MONDAL D.P., SAWLA S., RAMKRISHNAN N., Synergic effect of reinforcement and heat treatment on the two body abrasive wear of an Al-Si alloy under varying loads and abrasive sizes, *Wear*, **264**(1-2): 47-59, 2008, doi: 10.1016/j.wear.2007.01.039.
2. FRAGOMENI J.M., Characterization the brittle fracture and the ductile to brittle transition to ductile transition of heat-treated binary aluminum-lithium alloys, *Engineering Transactions*, **49**(4): 573-598, 2001.

3. KUMAR A., SASIKUMAR C., Effect of vanadium addition to Al-Si alloy on its mechanical, tribological and microstructure properties, *Materials Today: Proceedings*, **4**(2 – Part A): 307–313, 2017, doi: 10.1016/j.matpr.2017.01.026.
4. HURTALOVA L., TILLOVA E., CHALUPOVA M., The structure analysis of secondary (recycled) AlSi₉Cu₃ cast alloy with and without heat treatment, *Engineering Transactions*, **61**(3): 197–218, 2013.
5. NIKANOROV S.P., VOLKOV M.P., GURINT V.N., BURENKOV YU.A., DERKACHENKO L.I., KARDASHEV B.K., REGEL L.L., WILCOX W.R., Structural and mechanical properties of Al-Si alloys obtained by fast cooling of a levitated melt, *Materials Science and Engineering: A*, **390**(1–2): 63–69, 2005, doi: 10.1016/j.msea.2004.07.037.
6. KAISERA M.S., SABBIR S.H., KABIR M.S., SOUMMO M.R., AL NUR M., Study of mechanical and wear behaviour of hyper-eutectic Al-Si automotive alloy through Fe, Ni and Cr addition, *Materials Research*, **21**(4): 1–9, 2018, doi: 10.1590/1980-5373-MR-2017-1096.
7. APELIAN D., *Aluminum Cast Alloys: Enabling Tools for Improved Performance*, North American Die Casting Association, New York, 2009.
8. JORSTAD J., APELIAN D., Hypereutectic Al-Si alloys: practical casting considerations, *International Journal of Metalcasting*, **3**(3): 13–36, 2009, doi: 10.1007/bf03355450.
9. HIRSCH J., Aluminium in innovative light-weight car design, *Materials Transactions*, **52**(5): 818–824, 2011, doi: 10.2320/matertrans.l-mz201132.
10. STOJANOVIC B., BUKVIC M., EPLER I., Application of aluminum and aluminum alloys in engineering, *Applied Engineering Letters*, **3**(2): 52–62, 2018, doi: 10.18485/aeletters.2018.3.2.2.
11. BASAVAKUMAR K.G., MUKUNDA P.G., CHAKRABORTY M., Influence of melt treatments on sliding wear behavior of Al–7Si and Al–7Si–2.5Cu cast alloys, *Journal of Materials Science*, **42**(18): 7882–7893, 2007, doi: 10.1007/s10853-007-1633-7.
12. TAGHIABADI R., GHASEMI H.M., SHABESTARI S.G., Effect of iron-rich intermetallics on the sliding wear behavior of Al-Si alloys, *Materials Science and Engineering: A*, **490**(1–2): 162–170, 2008, doi: 10.1016/j.msea.2008.01.001.
13. ABDUL-LATIFF N.E., SUBHI A.D., HUSSEIN M.B., Effect of hot deformation on the wear behavior of Al₂O₃/A356 nano-composites, *Modern Applied Science*, **9**(11): 153–160, 2015, doi: 10.5539/mas.v9n11p153.
14. SAHEB N., LAOUI T., DAUD A.R., HARUN M., RADIMAN S., YAHAYA R., Influence of Ti addition on wear properties of Al-Si eutectic alloys, *Wear*, **249**(8): 656–662, 2001, doi: 10.1016/s0043-1648(01)00687-1.
15. ZEREN M., KARAKULAK E., Influence of Ti addition on the microstructure and hardness properties of near-eutectic Al-Si alloys, *Journal of Alloys and Compounds*, **450**(1–2): 255–259, 2008, doi: 10.1016/j.jallcom.2006.10.131.
16. GAO T., LI P., LI Y., LIU X., Influence of Si and Ti contents on the microstructure, microhardness and performance of TiAlSi intermetallics in Al-Si-Ti alloys, *Journal of Alloys and Compounds*, **509**(31): 8013–8017, 2011, doi: 10.1016/j.jallcom.2011.05.032.
17. GHOMASHCHI R., The evolution of AlTiSi intermetallic phases in Ti-added A356 Al-Si alloy, *Journal of Alloys and Compounds*, **537**: 255–260, 2012, doi: 10.1016/j.jallcom.2012.04.087.

18. KIM J.H., LEE K.M., LEE H.D., LEE T.G., PARK H.M., PARK H.D., Effects of titanium and boron additions with mechanical stirring on mechanical properties in Al-Si alloys, *Materials Transactions*, **56**(3): 450–453, 2015, doi: 10.2320/matertrans.l-m2014848.
19. CHINTHA A.R., Metallurgical aspects of steels designed to resist abrasion, and impact-abrasion wear, *Materials Science and Technology*, **35**(10): 1133–1148, 2019, doi: 10.1080/02670836.2019.1615669.
20. SHIVANATH R., SENGUPTA P.K., EYRE T.S., Wear of aluminium-silicon alloys, *The British Foundrymen*, **70**(12): 349–356, 1977.
21. ZUM GAHR K.H., Microstructure and wear of materials, Ch. 6. Sliding wear, *Tribology Series*, **10**: 351–495, 1987, doi: 10.1016/S0167-8922(08)70724-7.
22. CLARKE J., SARKAR A.D., Topographical features observed in a scanning electron microscopy study of aluminium alloy surfaces in sliding wear, *Wear*, **69**(1): 1–23, 1981, doi: 10.1016/0043-1648(81)90309-4.

Received March 4, 2020; accepted version August 29, 2020.

Published on Creative Common licence CC BY-SA 4.0

